



Evaluation of environmental factors related to *Aspergillus fumigatus* azole resistance in the Netherlands

Massimo Cogliati^{a,*}, Jochem B. Buil^b, Maria Carmela Esposto^a, Anna Prigitano^a,
Luisa Romano^a, Willem J.G. Melchers^b

^a Dept. Biomedical Sciences for Health, Università degli Studi di Milano, Milano, Italy

^b Dept. Medical Microbiology, Radboud University Medical Center, Nijmegen, the Netherlands

HIGHLIGHTS

- Azole resistance emergence risk is influenced by climatic more than anthropic factors.
- A one-degree rise of spring mean temperature increases the risk index up to two folds.
- Legumes, orchards, greenhouses, and dump sites are associated to a medium-high risk.
- Use of azole fungicides is not directly correlated to an increase of the risk.
- Zeeland and Noord-Holland are the provinces with the highest risk.

GRAPHICAL ABSTRACT



ARTICLE INFO

Editor: Kyle Bibby

Keywords:

Aspergillus fumigatus
Spatial analysis
Azole resistance
Fungicides
Environmental factor

ABSTRACT

Emergence of azole-resistant *Aspergillus fumigatus* represents a concern for public health worldwide. Here we applied a spatial analysis to a large number of records on *A. fumigatus* azole resistance in the Netherlands to evaluate the relationship of a set of environmental factors with the emergence of resistant isolates and to identify the potential risk areas. A total of 1850 aspergillosis cases were included in the analysis: 1559 caused by wild-type (WT) and 291 by azole-resistant (RES) strains. High-resolution maps containing environmental variables (climate, crop cultivations) were used as layers for spatial analysis. QGIS software was used for transformation and calculation of layers, and visualizing maps, whereas MaxEnt software was used to perform spatial analysis. A separate distribution map for WT and RES was generated using each layer, then the ratio between RES and WT suitability was calculated, and a new map was generated showing the areas where suitability of RES was higher than WT (ratio > 1). Layers presenting areas with a ratio > 1 were then used for a further analysis including all these layers together to generate a final risk map, to identify the most contributing environmental variables, and to estimate the number of people potentially exposed to the risk. Results showed that the areas with the highest RES/WT ratio were associated with the following variables: legume cultivations ratio 1.5–2.7; fruit tree plantations, ratio 2.1; dump sites and artificial sites, ratio 2.3–2.7; spring minimum and mean temperatures, ratio 1.6–1.8. Areas with medium, high, and very high risk covered a surface of about 2330 km² and people exposed

* Corresponding author at: Lab. Micologia Medica, Dip. Scienze Biomediche per la Salute, Università degli Studi di Milano, Via Pascal 36, 20133 Milano, Italy.
E-mail address: massimo.cogliati@unimi.it (M. Cogliati).

<https://doi.org/10.1016/j.scitotenv.2024.177923>

Received 6 September 2024; Received in revised form 12 November 2024; Accepted 2 December 2024

Available online 6 December 2024

0048-9697/© 2024 The Authors. Published by Elsevier B.V. This is an open access article under the CC BY-NC-ND license (<http://creativecommons.org/licenses/by-nc-nd/4.0/>).

were >319,000, with Zeeland and Noord-Holland being the provinces with the highest risk. All together these results suggest that azole-resistance emergence is a complex phenomenon depending on a multitude of environmental variables that are not yet been fully explored.

1. Introduction

Aspergillus fumigatus is an opportunistic human fungal pathogen responsible for over 250,000 cases of invasive aspergillosis and three million cases of chronic pulmonary aspergillosis worldwide each year among immunocompromised individuals. The mortality rate can reach as high as 90 % when antifungal resistance occurs (Bongomin et al., 2017; WHO, 2022). Given this epidemiological landscape, the World Health Organization has classified *A. fumigatus* as one of the four most critical fungal pathogens posing a significant public health concern (WHO, 2022).

Aspergillus fumigatus is a ubiquitous environmental fungus predominantly present in soil, plant debris, and compost materials. It produces abundant conidiospores which are able to disperse in the environment through air, water or animal carriers, making them easily inhalable by hosts, particularly when their immune systems are compromised (Kwon-Chung and Sugui, 2013). The primary therapy for treatment of invasive aspergillosis relies on azole antifungals such as voriconazole, posaconazole, and itraconazole (Heylen et al., 2024). However, in the past two decades, the effectiveness of these antifungals has been jeopardized by the emergence of multi-azole resistant strains of *A. fumigatus* (Verweij et al., 2009; Bosetti and Neofytos, 2023). The initial concern regarding azole-resistant aspergillosis cases was reported in the Netherlands where the percentage of cases increased from 0 % prior to 2000 to 12 % in 2009 (Snelders et al., 2008; van der Linden et al., 2011). Since then, *A. fumigatus* resistant strains were isolated from aspergillosis cases and environment worldwide representing a serious public health problem (Chowdhary et al., 2013; Amona et al., 2022; De Francesco, 2023; Lockhart et al., 2023; Lin et al., 2023). Furthermore, a recent review examined the spatiotemporal evolution of antifungal resistance distribution worldwide, revealing an alarming parallel increase in reports of both crop and human infections caused by resistant strains (Fisher et al., 2018). The primary mechanisms involved in *A. fumigatus* azole resistance include point mutations in the *CYP51A* gene, which is crucial for ergosterol biosynthesis, and replications of its promoter. Among these, the TR34/L98H mutants are the most frequently identified in both clinical and environmental isolates (Snelders et al., 2008). This suggested the hypothesis that resistance is induced by specific environmental stress and selected genetically due to the widespread use of azole fungicides in agricultural practices (Verweij et al., 2009; Kang et al., 2022). This aligns with the agricultural context where the phenomenon was first observed, being the Netherlands the main European country in terms of fungicide usage on crops.

Some studies have reported the isolation of resistant *A. fumigatus* strains from agricultural soil treated with fungicides, however comparison with the prevalence of these strains in untreated soils have not shown significant differences in most cases (Kemoi et al., 2017; Godeau et al., 2023; Chen et al., 2024; Celia-Sanchez et al., 2024). Furthermore, some other questions remain open about emergence of azole resistance in *A. fumigatus*. Resistant strains have been identified in remote geographical areas far from agricultural areas, such as from a Chinese Himalayan region and from arctic soils of Canada, suggesting either long-distance dispersal of resistant spores or spontaneous occurrence of the azole resistance mutations *in situ* (Korfanty et al., 2021; Zhou et al., 2023; Shelton et al., 2023). In addition, a small percentage of *A. fumigatus* azole-resistant isolates do not harbor a mutation in the *CYP51A* gene suggesting that other mechanisms inducing resistance might be involved (He et al., 2024). Finally, the coexistence of resistant and wild-type strains in the same environment underscores the need to assess the risk of infection by a resistant strain in a specific geographical

area.

Although *A. fumigatus* azole-resistant strains were isolated in the Netherlands environment in specific geographic hotspots and sources (Schoustra et al., 2019), an extensive environmental survey has yet to be conducted. Therefore, data concerning their geographical distribution and prevalence compared to wild-type strains are not available. This lack of data also hinders the identification of potential environmental factors that could influence the emergence of azole resistance. Recently, spatial analysis has emerged as an interesting holistic approach to predict the geographical distribution of various species, including microorganisms, and to identify their relationship with a multitude of environmental factors (Phillips et al., 2006). In the present study, we applied such an approach to analyze extensive data collected in the Netherlands regarding *A. fumigatus* azole resistance, aiming to evaluate the relationship between a set of environmental factors and the emergence of resistant isolates, as well as to identify the potential risk areas within the country.

2. Materials and methods

2.1. Cases of aspergillosis

A total of 1850 clinical cases of aspergillosis due to *A. fumigatus sensu stricto*, recorded in the Netherlands from 2019 to 2022, were included in the analysis. Cases in which azole resistance developed after azole therapy were excluded. Wild-type (WT) *A. fumigatus* were isolated from 1559 cases, whereas azole-resistant (RES) strains from 291 cases. Most of the cases due to RES strains (190/291, 65 %) were confirmed by sequencing of *CYP51A* gene. TR34/L98H mutation was detected in 146 isolates and TR46/Y121F in 44 isolates (Supplementary Table S1).

2.2. Georeferencing of the cases

Each case was associated with a two-digit postal code corresponding to a restricted geographical area where the patient was resident. Postal code map was obtained by Postcodebijdadres website (<https://postcodebijdadres.nl/postcodes-nederland>). To assign geographic coordinates to each case, random points were generated within the corresponding postal code areas using the option “random points from a polygon” of the QGIS software (<https://www.qgis.org/it>) (Supplementary Fig. S1). Two separate files, one containing the coordinates of the cases due to WT cases and one containing those due to RES cases, were prepared for subsequent analyses.

2.3. Environmental variable datasets

High-resolution raster maps containing a set of environmental variables were retrieved and downloaded from online sources (Supplementary Table S2). Climate datasets included monthly minimum temperatures, monthly maximum temperatures, monthly average temperatures, and monthly precipitations, recorded from 2011 to 2021 in Europe. Two maps reporting the spatial distribution and the type of crops cultivated in the Netherlands were downloaded from European Space Agency (ESA) and Joint Research Centre Data of European Union (EU). The ESA map reported data recorded in 2017 and the EU map 2018 data. Most of the main crops were reported in both the maps and some others were differently reported in the two maps. From Copernicus website we also downloaded a dataset map containing data of land use in Europe. Finally, a high-resolution map reporting the population density in the Netherlands was used to estimate the number of people

potentially exposed to azole-resistant *A. fumigatus* strains. The geographical area considered for the analysis covered the entire Netherlands, and all raster maps were clipped, by QGIS software, to the following coordinates: longitude 3.36–8.38, latitude 50.75–54.32. The raster size was also homogenized to a final resolution of $8636 \times 10,207$ cells, converted to WGS84 geographical projection, and finally saved in ASCII format.

2.4. Spatial analysis

Spatial analysis was performed using the open-source software MaxEnt (Phillips et al., 2006). The analysis requires two types of data: a list of occurrence points, including the geographic coordinates of the aspergillosis cases, and one or more dataset layers, corresponding to raster maps reporting the distribution of values for one or more environmental variables. The algorithm calculates the probability of presence (suitability) of the target category of occurrence points for each value of the variables at each cell of the resulting raster map. The analysis produces also a set of response curves displaying how the probability of presence for a group of occurrence points varies in respect of the values of the analyzed variables. The weight of each raster layer to infer the final distribution model was calculated by jackknife analysis implemented in the MaxEnt software. The reliability of the distribution model produced by the algorithm was determined by the area under the curve (AUC) which measures how the model prediction differs from a random prediction (AUC = 0.5).

For each of the five set of variables (climate datasets, ESA crop dataset, EU crop dataset, land use dataset, and population density dataset) two separate spatial analysis was performed, one for WT occurrence points and one for RES occurrence points. The resulting WT and RES suitability raster maps were imported into QGIS software and the ratio of the probability values, RES/WT, for each cell of the raster was calculated. The output was a new raster map displaying the distribution of ratio values. The areas with a ratio value >1 corresponded to the areas where the probability of the azole resistance emergence was higher than the probability of presence for WT.

Datasets that produces a ratio maps containing areas with values >1 were considered for the final analysis whereas the others were discarded. The selected datasets were therefore imported all together into Maxent software and the analysis was repeated as described above. The final distribution map of RES/WT ratio values was inferred and used for the next steps.

2.5. Risk map implementation

The RES/WT ratio values of the final distribution map were grouped into six categories: <0.1 = no risk, $0.1 - < 1.1$ = very low risk, $1.1 - < 1.5$ = low risk, $1.5 - < 1.7$ = medium risk, $1.7 - 2.0$ = high risk, >2.0 = very high risk. Each range of values was then substituted by the risk class using the option “raster calculator” of QGIS software, and finally visualized with different colors.

2.6. Analysis of the main contributing variables

The variables that most significantly contributed to infer the final risk map were further analyzed to assess their relationship with the risk for azole resistance emergence. The risk map raster was imported in QGIS software and the raster of each of the variables was used as zonal layer to calculate zonal statistics using the option “zonal statistics of the raster”. For categorical variables the algorithm calculated the mean of the WT/RES ratio values for each category present in the zonal layer, and then the results were visualized as a histogram reporting bar of different colors corresponding to the risk classes. For continuous variables the algorithm calculated the mean of the WT/RES ratio values for all the variable values present in the zonal layer, then the results were ordered based on the variable values and plotted in a graphic were the

risk is a function of the variable. From the graphics it was possible to determine the range of values of the variable associated with a specific class of risk.

2.7. Estimation of the territory surface and the number of people potentially exposed to the risk

Number of people living in the areas identified by the spatial analysis model as potentially at risk for emergence of azole resistance was determined overlapping the risk map raster inferred above, with the population density map, using the option “zonal statistics of the raster” in the QGIS software. The sum of the values of all cells included in each risk class area corresponded to the number of people living in that area.

Similarly, the surface covered by each risk class area was calculated overlapping the risk map raster with a raster map of the Netherlands surface. In this case the count of the raster cells included in each risk class area multiply for the area covered by one single cell corresponded to the surface covered by each risk class.

The population and surface area exposed to the different classes of risk were also calculated for each of the 12 provinces of the Netherlands.

2.8. Distribution map of azole fungicides usage in agriculture and estimation of azole resistance emergence risk

We tried to estimate the risk of azole resistance emergence by directly correlating occurrence data of the cases here reported with a distribution map of azole fungicide usage in Dutch agriculture. Such a map is not available at present and therefore we tried to infer it using the database of the Centraal Bureau voor de Statistiek (CBS, <https://opendata.cbs.nl/statline/#/CBS/nl/dataset/84010NED/table?dl=1CE23>). The database reports the annual quantity/ha (as for 2016) of several fungicides used in agriculture, classified by crop type. Among the listed fungicides are 12 azole derivatives and namely: bromuconazole, cyproconazole, difenoconazole, epoxiconazole, etridiazole, metconazole, penconazole, propiconazole, prothioconazole, tebuconazole, thia-bendazole, and triflumizole. The annual quantity/ha of these fungicides were downloaded and the average value was calculated for each of the following crops: maize, sugar beet, summer wheat, summer barley, carrot, dry pulses, winter wheat, potatoes, onion, tulip, fruit trees, and *Lilium*. Since the geographical distribution of these crops are reported in the ESA crops map, the corresponding values in the raster cells were substituted by the annual quantity/ha of the azole fungicides using the option “raster calculator” of QGIS software, transforming the raster map in a distribution map of azole fungicides usage. The new raster was then input as dataset layer into MaxEnt software and analyzed with WT and RES occurrence points as described above.

2.9. Determination of dispersion routes for azole resistant *A. fumigatus*

Dispersion of *A. fumigatus* in the environment is primarily due to production of conidia that can be transported by wind, water, animals, and human activities over long distances. To determine the potential dispersion routes for the azole-resistant strains we assumed that distance between two occurrence point is directly proportional to their distance from the origin of dispersion. Therefore, we selected a set of occurrence points including only cases due to TR34/L98H resistant strains (146 cases), we generated a distance matrix for all points by Geographic Distance Matrix Generator software v1.2.3 (Center for Biodiversity and Conservation at the American Museum of Natural History, New York, USA), and then we formatted the matrix in .meg format to generate a neighbor-joining tree using MEGA software (<https://www.megasoftware.net>). The geographic coordinates of the points in each of the main branch of the tree were identified and grouped as separate sets of occurrence points. Each branch of the tree represented a potential dispersion route being the points near the origin of each branch the origin of the dispersion, with points closer to the branch origin

representing the earliest stages of dispersion. The occurrence points along each dispersion route (tree branches) were displayed on the risk map inferred above and the different flows of dispersion were represented by arrows connecting the origin with the more distant points.

3. Results

3.1. Spatial analysis of the different set of raster layers

All distribution models generated by spatial analyses of the different datasets were considered reliable, as the AUC values exceeded 0.65, with the AUC calculated for the climate model being the highest at 0.84 (Supplementary Table S3).

Spatial analysis considering all 48 climatic raster layers produced two distinct distribution models for WT and RES occurrence points (Fig. 1A-B). In both models, areas with high and low probability of presence were identified and then compared by calculating the RES/WT probability ratio. The ratio map showed four areas with values >1 located in northwest, southwest, northeast and southeast of the Netherlands (Fig. 1C). The main variables contributing to the model, as identified by jackknife analysis, were the average of mean and minimum temperatures during spring and, with a minor contribution from precipitations during late spring (Fig. 1D). Further analysis of climatic variables showed that an increase of temperatures across all seasons of the year was associated with a rise in the RES/WT ratio

(Supplementary figs. S2-S4). In contrast, no similar trend was observed for precipitation variables, except for precipitations in May, where the ratio slightly increased with values in the range from 58 to 70 mm (Supplementary fig. S5).

Spatial distribution of probability of presence for WT and RES, based on the ESA crop map as raster layer, showed suitability values >0.5 for all crops represented in the raster (Fig. 2A-B). However, when RES/WT ratio was calculated, only a few crop variables presented a ratio value >1 : clover root, *Medicago*, *Lilium*, maize, and sugar beet. The model did not identify specific areas with high ratio values since they were distributed in all the Netherlands territory (Fig. 2C-D).

Similarly, analysis performed using the EU crop map generated WT and RES distribution maps with probability values >0.5 for most of the Netherlands (Fig. 3A-B). The RES/WT ratio map showed a ratio >1 for dry pulses, durum wheat, rape, barley, maize, and artificial areas. This crop landscape was distributed mostly in the northern and southern regions and, in a minor extent, in the central areas (Fig. 3C-D).

A correlation was also found between some land use variables and the RES/WT ratio values in the predicted distribution model. Ratio values >1 were calculated for seven variables classified as water bodies, airports, fruit trees, dump sites, construction sites, sport and leisure sites, and complex cultivations, which were distributed mostly in the southern and eastern part of the country (Fig. 4A-D).

A different result was obtained when population density layer was uploaded for spatial analysis. The two resulting distribution maps for

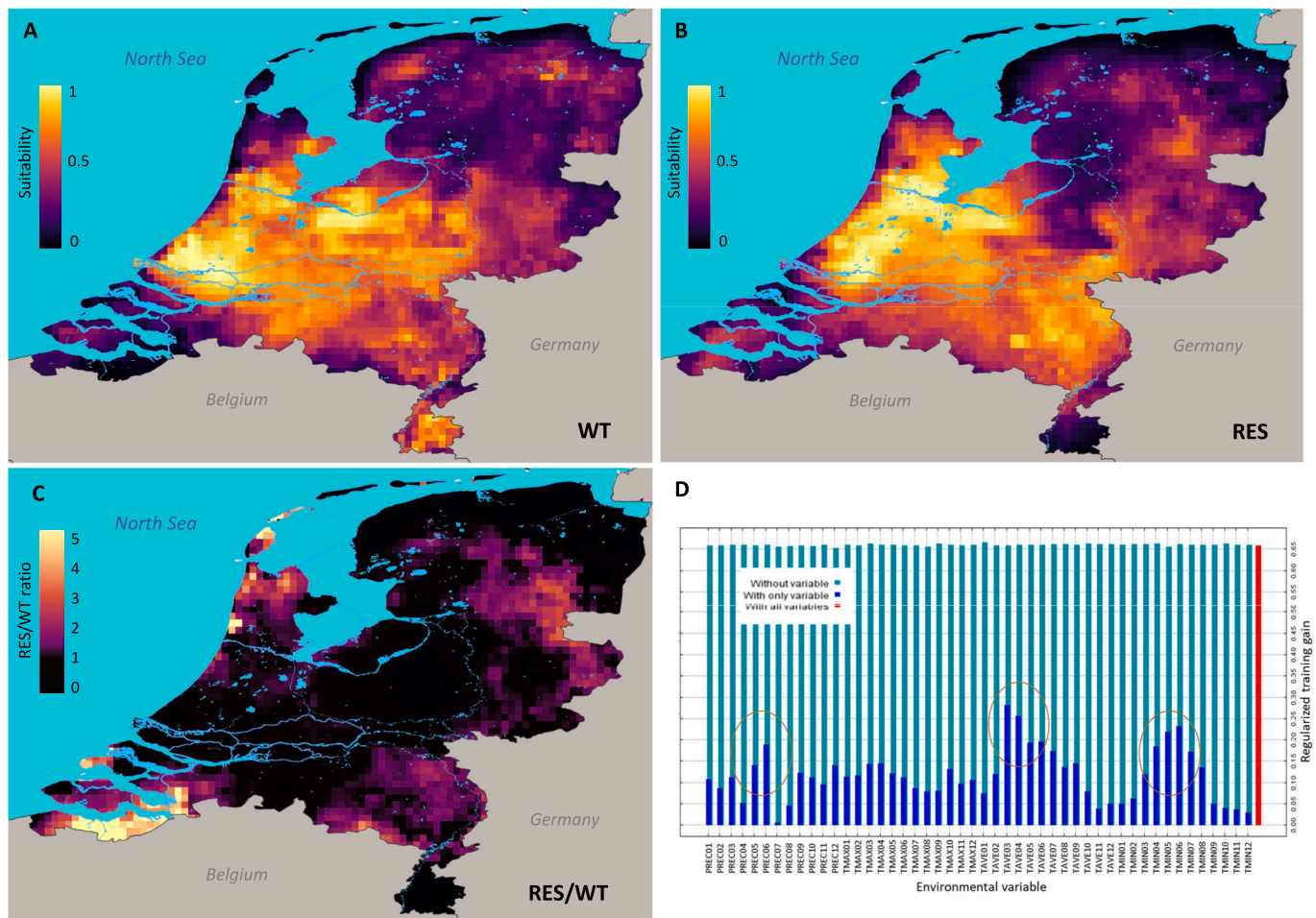


Fig. 1. Distribution model based on 48 climatic dataset layers (monthly precipitations, PREC; monthly maximum temperatures, TMAX; monthly average temperatures, TAVE; monthly minimum temperatures, TMIN) inferred for A) wild-type occurrence points (WT) and B) resistant occurrence points (RES). C) Distribution map inferred calculating the ratio between RES and WT distribution probabilities. D) Jackknife analysis of the main contributing variables to the model. Red circles identify the most contributing variables.

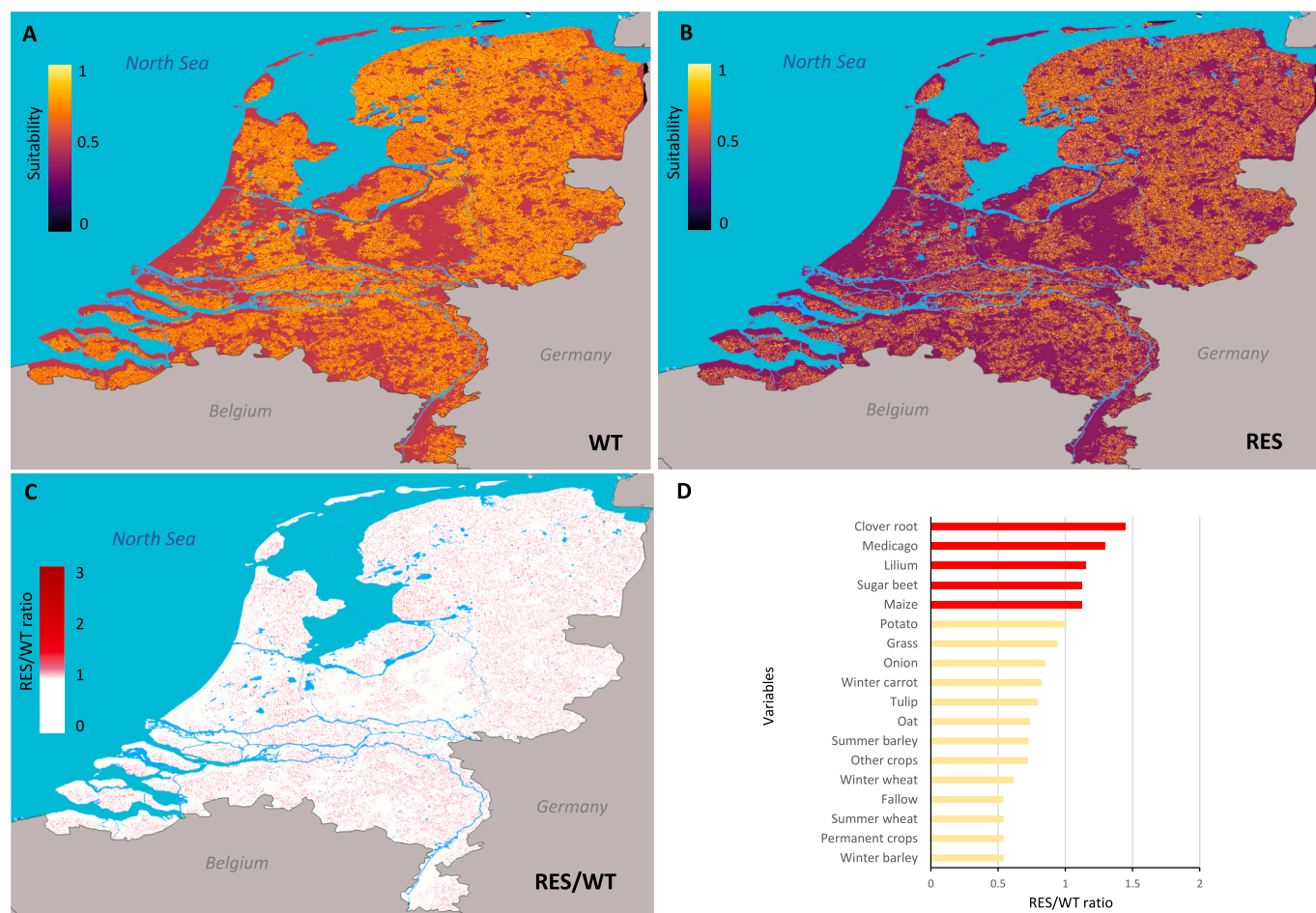


Fig. 2. Distribution model based on 18 categorical variables included in the ESA crops layer inferred for A) wild-type occurrence points (WT) and B) resistant occurrence points (RES). C) Distribution map inferred calculating the ratio between RES and WT distribution probabilities. D) Values of RES/WT ratio calculated for each variable. Red bars indicate values >1 and yellow bars values ≤ 1 .

WT and RES occurrence points were very similar and therefore the RES/WT ratio map did not identify sufficient raster cells containing values >1 (Supplementary figs. S6A–C). Further analysis did not suggest any correlation between population density and an increase in the ratio values (Supplementary fig. S6D).

3.2. Final spatial analysis with the main raster layers

Based on the results described above, nine raster layers were selected for final spatial analysis: monthly precipitations in May and June, monthly minimum temperatures in May and June, monthly average temperatures in March and April, ESA crop raster, EU crop raster, and land use. Fig. 5A and B show the probability distribution for WT and RES occurrence points obtained by the final analysis. Although the WT distribution model showed a more extensive area presenting high probability values than RES distribution model, the RES/WT ratio map displayed two main areas with ratio values >1 located in the Noord-Holland and Zeeland provinces. Other areas highlighted by the model, but with a lower intensity, were the western, southern and eastern part of the country (Fig. 5C). The risk map inferred from the RES/WT ratio model confirmed that the two areas described above included also the areas with the highest risk categories. High and medium risk areas were also detected in the northern part of Zuid-Holland, western part of Noord-Brabant, and Limburg, as well as sparsely in the other provinces except Utrecht province (Fig. 5D).

Analysis of the main contributing climatic variables showed no correlation between precipitations and an increase of RES/WT ratio

(Fig. 6A-B). In contrast, the average of mean temperatures in March were positively correlated with an increase in risk: areas with an average temperature above $6.3\text{ }^{\circ}\text{C}$ were associated with a rapid rise in the risk level, reaching medium and high-risk classes when temperatures exceeded $6.5\text{ }^{\circ}\text{C}$ (Fig. 6C-D). The same trend was observed analyzing the average minimum temperatures in May and June with critical temperatures thresholds at $9.3\text{ }^{\circ}\text{C}$ and $12.4\text{ }^{\circ}\text{C}$, respectively, marking the transition to medium-risk levels (Fig. 6E-F).

Among the categories included in the two analyzed crop maps, five categories resulted associated with a significant level of risk. The categories “dry pulses” and “other industrial crops” were associated with a medium risk, clover root cultivation to a high risk, and *Medicago* cultivations and “artificial areas” to a very high risk. (Fig. 7A-B).

Finally, among the categories included in the land use raster only two categories were associated with a very high-risk class, “fruit tree and berry plantations” and “dump sites” (Fig. 7C).

3.3. Territory and population exposed to the risk

The Netherlands areas exposed to medium, high, and very high risk covered a surface of about 2330 km^2 , representing 5.57 % of the country's territory. The largest portion of this area was located in Zeeland (2.6 %), Noord-Holland (1.44 %), Noord-Brabant (0.39 %), and Zuid-Holland (0.35 %), with the remaining provinces having $<0.2\%$ of their territory exposed to risk (Supplementary Table S4 and Fig. 8A).

Number of people exposed to medium, high, and very high risk was over 319,000, representing 1.82 % of the population of the Netherlands.

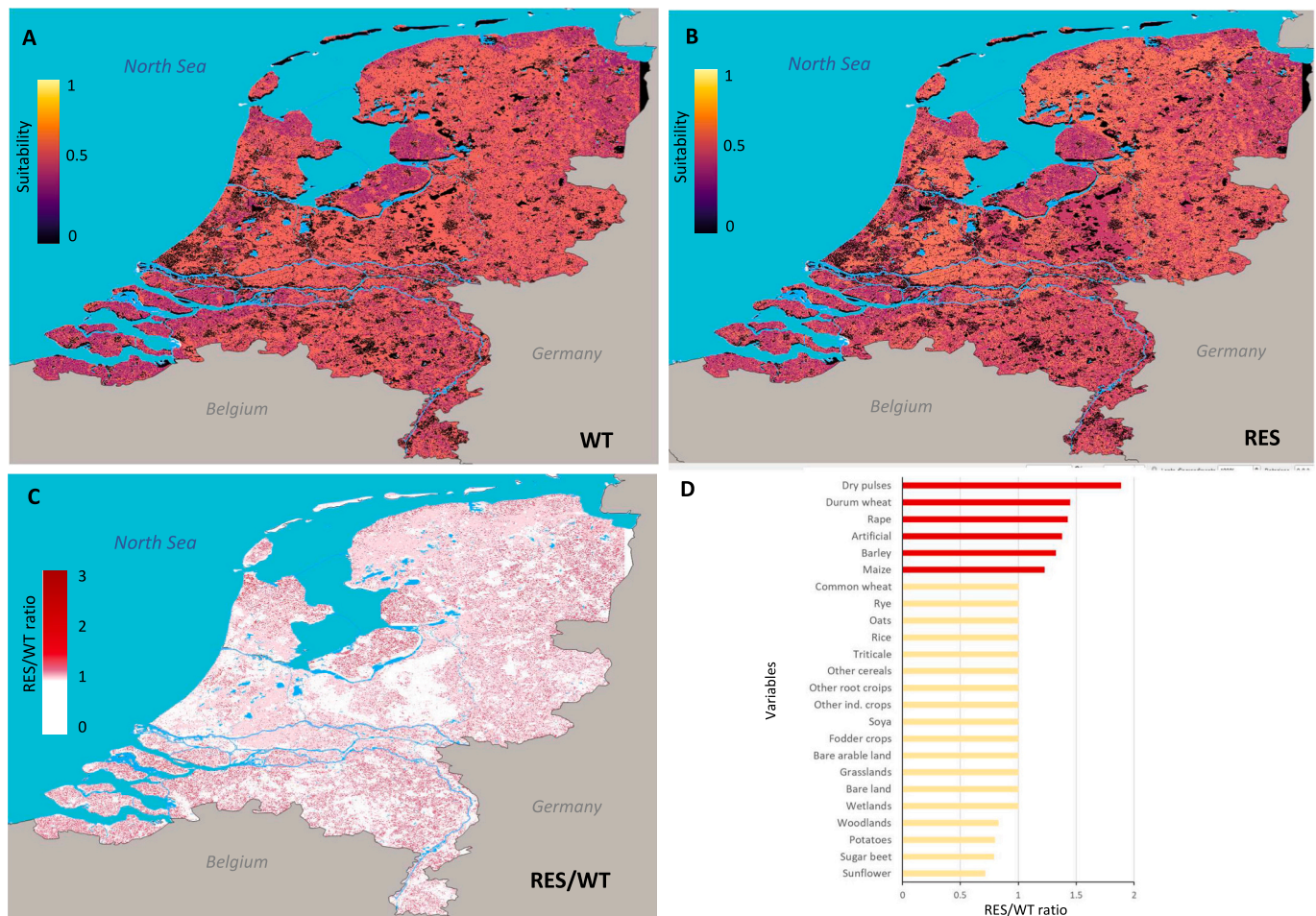


Fig. 3. Distribution model based on 24 categorical variables included in the EU crops layer inferred for A) wild-type occurrence points (WT) and B) resistant occurrence points (RES). C) Distribution map inferred calculating the ratio between RES and WT distribution probabilities. D) Values of RES/WT ratio calculated for each variable. Red bars indicate values >1 and yellow bars values ≤1.

Zeeland and Noord-Holland had the highest number of people at risk (116,644 and 89,706, respectively) (Supplementary Table S5 and Fig. 8B).

3.4. Emergence of azole resistance and azole fungicide use in agriculture

Data extrapolated from the CBS database concerning the use of fungicides in various crops showed that the highest quantities of fungicides, including azole derivatives, were applied to flower cultivations followed by fruit tree plantations, potatoes, and onion (Fig. 9A). The distribution map of azole fungicide usage in the Netherlands, inferred combining CBS data and ESA crop map, is shown in Fig. 9B. Four areas, where azole fungicides are largely used, were identified: Zeeland, northern Noord-Holland, Flevoland, and the northeastern part of the country. The spatial analysis performed uploading the above layer with WT and RES occurrence points resulted in two probability distribution maps that were very similar, and the RES/WT ratio map did not identify any areas with values >1. As a result, the whole territory was classified as low risk for *A. fumigatus* azole resistance in relation to the use of azole fungicides (Fig. 9C-D).

3.5. Dispersion routes of *Aspergillus fumigatus* TR34/L98H mutants

The analysis, performed as described in materials and methods, identified four potential routes of dispersion for *A. fumigatus* TR34/L98H mutants (Fig. 10). Route 1 originated from eastern Utrecht province and then dispersed towards western and northern provinces. Route 2

originated from western Utrecht province and spread southeastward. Route 3 originated in Zuid-Holland near Rotterdam and dispersed towards southwestern provinces. Finally, route 4 originated near Amsterdam and dispersed towards northern part of Noord-Holland province, as well as towards Zuid-Holland and Flevoland. Although, the points of origin of all the routes were located in areas classified as low or very low risk, for routes 2, 3, and 4, the most distant points of dispersion from the origins were located in areas classified as very high, high, or medium risk, as identified by spatial analysis.

3.6. Limitations of the present analysis

The above results could have been biased by a number of factors. One could be represented by data collection. We recorded 1850 cases of aspergillosis but this number could represent an underestimation of the cases, particularly for cases due to wild-type strain since the study was focused on azole resistance. Cases were associated with a postal code but the exact locations of patients' residences were unknown, therefore a randomization was needed to assign an exact pair of coordinates to each case. However, the small geographic area of each postal code limits the bias. In addition, we assumed that the place of residence of the patient was the most probable place where the infection was acquired. Although this could be true for most of the cases, it can not be excluded that some patients were infected outside the residence place. Another limitation is the absence in this study of occurrence points related to environmental strains. Including environmental findings was not possible since, at present, environmental surveys in the Netherlands have not yet been

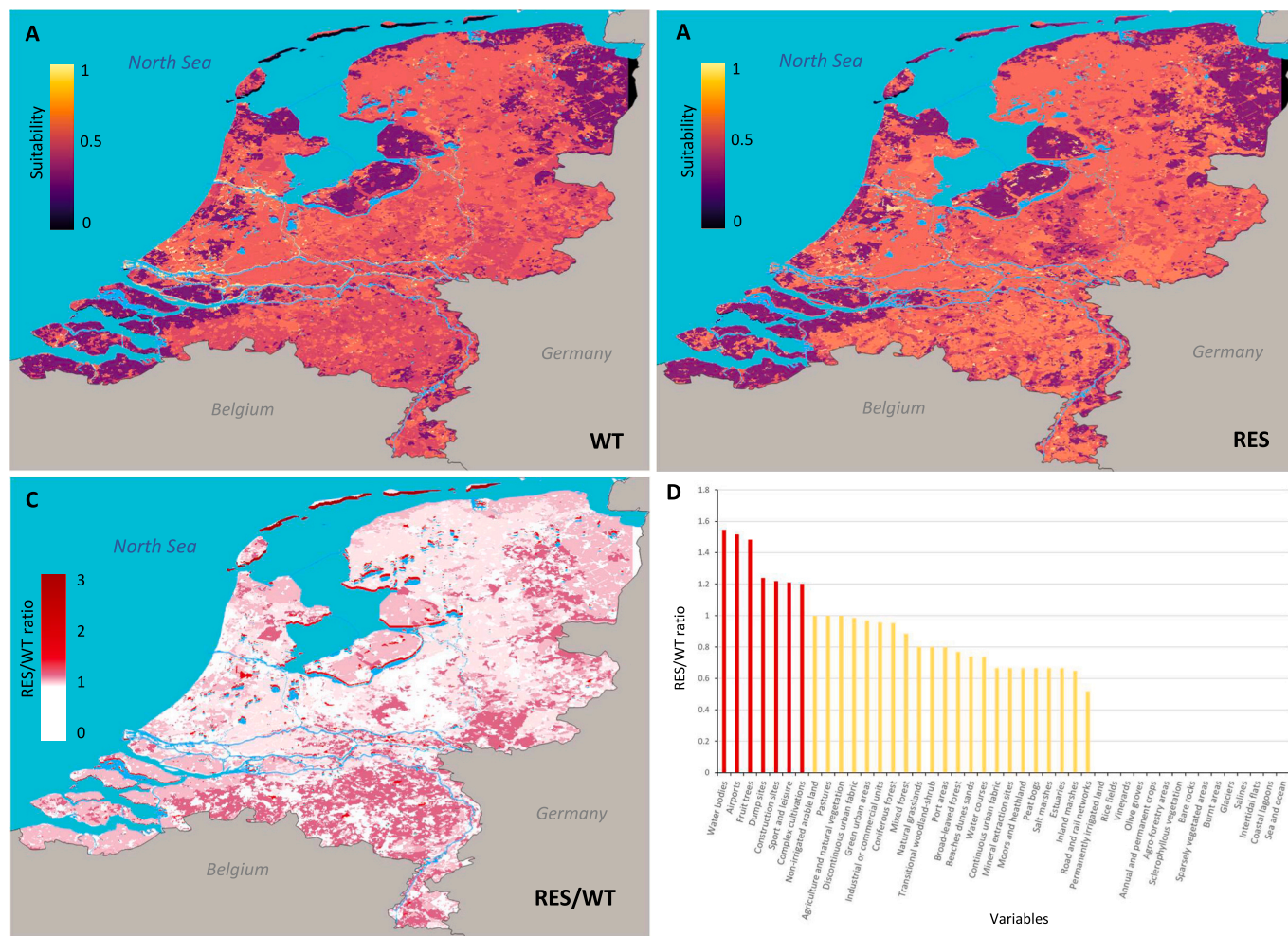


Fig. 4. Distribution model based on 44 categorical variables included in the land use layer inferred for A) wild-type occurrence points (WT) and B) resistant occurrence points (RES). C) Distribution map inferred calculating the ratio between RES and WT distribution probabilities. D) Values of RES/WT ratio calculated for each variable. Red bars indicate values >1 and yellow bars values ≤1.

carried out except for some collections in few hotspot places. As regards dataset layers, we selected a number of layers containing some environmental factors that could influence the emergence of azole resistance but, in future studies, other factors could be taken in consideration and this could lead to different results in respect of those obtained here. For instance, crops and land use layers contain punctual data referring to type and distribution of crops as well as land cover during a specific year and therefore they may change over different seasons and years. In the present analysis we used two crop maps referring to two different years to reduce this bias. Furthermore, the data on azole fungicide usage may be biased by the database source used for the analysis. The values recorded in this database depend on the voluntary declaration of the users and thus they could lack in reliability and completeness. Anyway, they are the best data publicly available. Finally, we inferred some potential routes of dispersion for TR34/L98H mutants based on a matrix of geographical distances between occurrence points, however we were able to include in the analysis only a part of the cases since not all the *A. fumigatus* isolates causing the infection were investigated to detect TR34/L98H mutations. In addition, the results here obtained would be better corroborated by a further genotyping analysis that was not performed.

4. Discussion

The results here reported represent a first attempt to correlate a

multitude of environmental factors and the emergence of *A. fumigatus* azole resistance in the Netherlands. Among the different factors analyzed, climatic conditions seem to be the most relevant compared to the others. Our distribution model showed that an increase of <1 °C in the average temperature during early spring leads to an increase of the risk index up to two folds, shifting a low-risk areas into medium- or high-risk zones. The average temperature resulted primarily influenced by minimum temperatures during spring, rather than maximum temperatures, suggesting that slight fluctuations of minimum temperatures can mostly impact on azole-resistance emergence in *A. fumigatus*. The advantage of azole-resistant *A. fumigatus* strains over wild-type strains in such climatic conditions may be explained by an increase of frequency of mutations or by an increased fitness of mutants. Relationship between azole-resistance emergence in *A. fumigatus* and environmental temperature is still not well understood. Some studies showed that composted plant debris provides a more favorable substrate than plant debris collected directly from agricultural or horticultural fields, suggesting that the warmer conditions in the compost environments may contribute to the high proliferation of *A. fumigatus*, thus increasing the likelihood of resistant mutants emerging (Pugliese et al., 2018; Shelton et al., 2022; Hanne et al., 2024). Our results are even more relevant if we consider the trend of global temperatures in the last century which has recorded an increase of about 1 °C (<https://data.giss.nasa.gov/gistemp>). Should this trend continue, it is likely that, based on our predictive model, the risk of infection by a resistant strain will rise in parallel with the

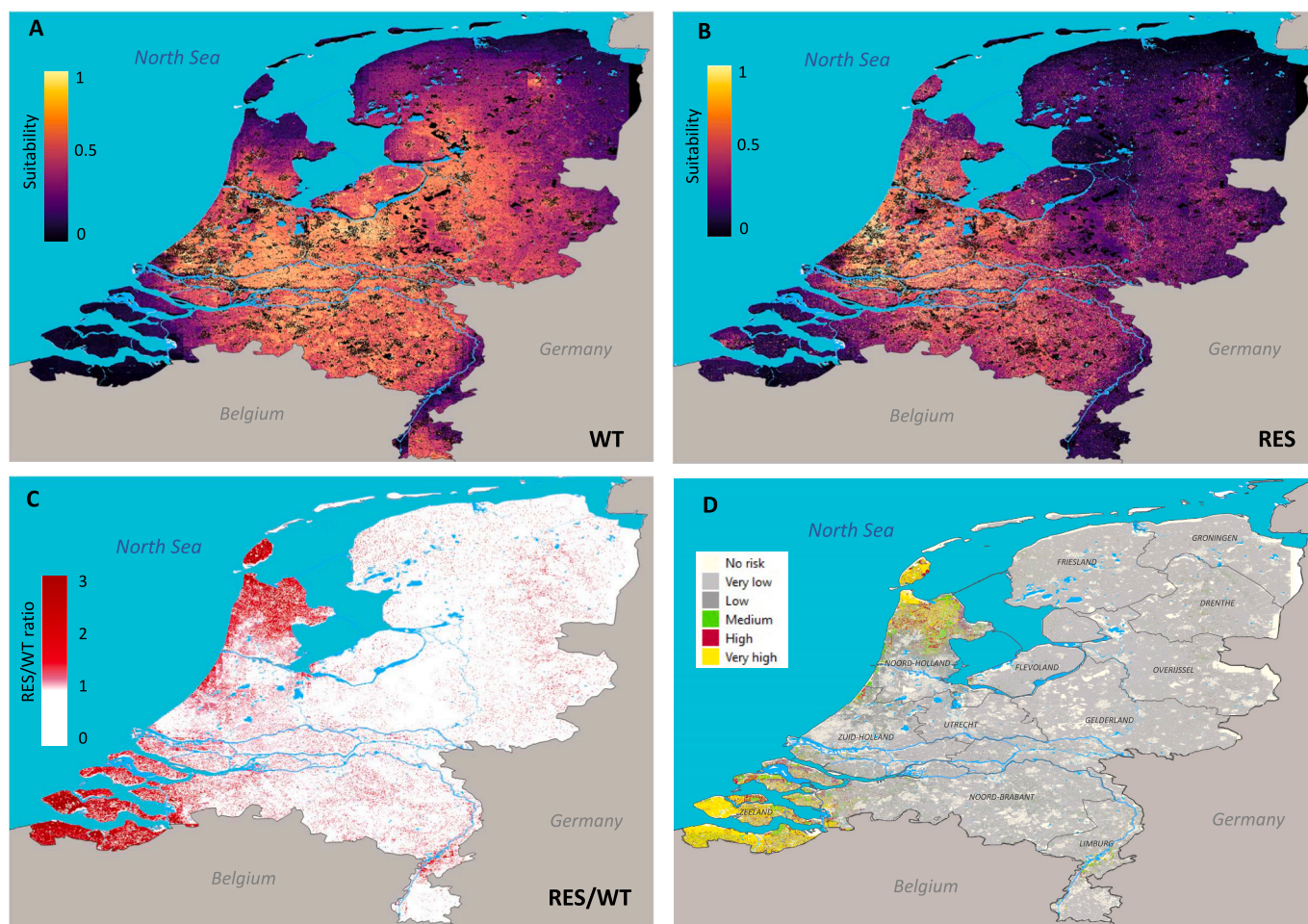


Fig. 5. Distribution model based on the most contributing layers (minimum temperature in May and June, average temperature in March and April, precipitations in May and June, EU crops map, ESA crops map, and land use map) inferred for A) wild-type occurrence points (WT) and B) resistant occurrence points (RES). C) Distribution map inferred calculating the ratio between RES and WT distribution probabilities. D) Map of the Netherlands showing high and low risk areas for the emergence of *Aspergillus fumigatus* azole resistance. Province boundaries are also shown.

expansion of high-risk areas. Interestingly, no correlation was found between precipitation levels and the emergence of azole resistance in this study. As the Netherlands is a relatively small country with rainfall distributed almost uniformly across the entire territory, the influence of this variable on the risk index was difficult to detect. An analysis carried out on a larger territory could better elucidate this issue.

Among the variables related to agricultural practices, our results show a strong correlation between areas presenting orchard cultivations and high-risk areas. This is in line with the hypothesis that soil treated with fungicides could contribute to higher prevalence of azole-resistant strains, as orchards typically require heavy fungicide applications to preserve fruits from molds attacks (Toda et al., 2021). However, studies on the prevalence of *A. fumigatus* in orchards soil are lacking except one isolation from northern Italy (Prigitano et al., 2014), meaning further investigation is needed.

Our distribution model identified the category named “artificial areas” as potentially high-risk areas. This category, among others, includes greenhouses which are widely diffuse in the Netherlands for cultivation of flowers and horticultural products (LUCAS 2018, Eurostat, <https://ec.europa.eu/eurostat/documents/205002/8072634/LUCAS2018-C3-Classification.pdf>). Greenhouse are controlled environment where the temperatures are higher than those outside, and fungicides can accumulate, potentially favoring the selection and proliferation of azole-resistant strains. Recent studies carried out in China confirm that, in greenhouses soils, prevalence and genetic

variability of *A. fumigatus* azole resistant strains is higher than in the natural environment, suggesting that greenhouses should be closely monitored as potential sources of antifungal resistance (Zhou et al., 2021, 2022).

Dump sites are other areas associated to a high-risk index in our model. In waste collection depots, leaves, plant retails, and grass are cumulated as big piles where *A. fumigatus* was showed to be able to proliferate abundantly (Kontro et al., 2022). Compost piles were also investigated for the presence of azole resistant strains and in most of the cases they resulted positive (Zhang et al., 2021; Gómez Londoño and Brewer, 2023; Wang et al., 2024; Hanne et al., 2024, Arendrup et al., 2024). In addition, in mixed waste areas where organic and inorganic waste are accumulated together, it is likely that *A. fumigatus* can interact with a range of chemical compounds, which may increase mutation rates.

Intensive cultivation of flowers is one of the most productive activities in the Netherlands with large areas planted with tulip and lilies. These flower cultivations require a constant treatment with fungicides due to the fragility of flowers and to preserve bulbs. Despite the high exposure to fungicides of these areas, interestingly, they were not associated with a high-risk index. The high dosage of fungicides employed to treat flowers could explain our results which reflect the efficacy of the fungicides to eradicate *A. fumigatus* from this kind of soil.

In contrast, areas cultivated with legumes (dry pulses, *Medicago*, and clover) were associated with medium or high-risk zones, even though

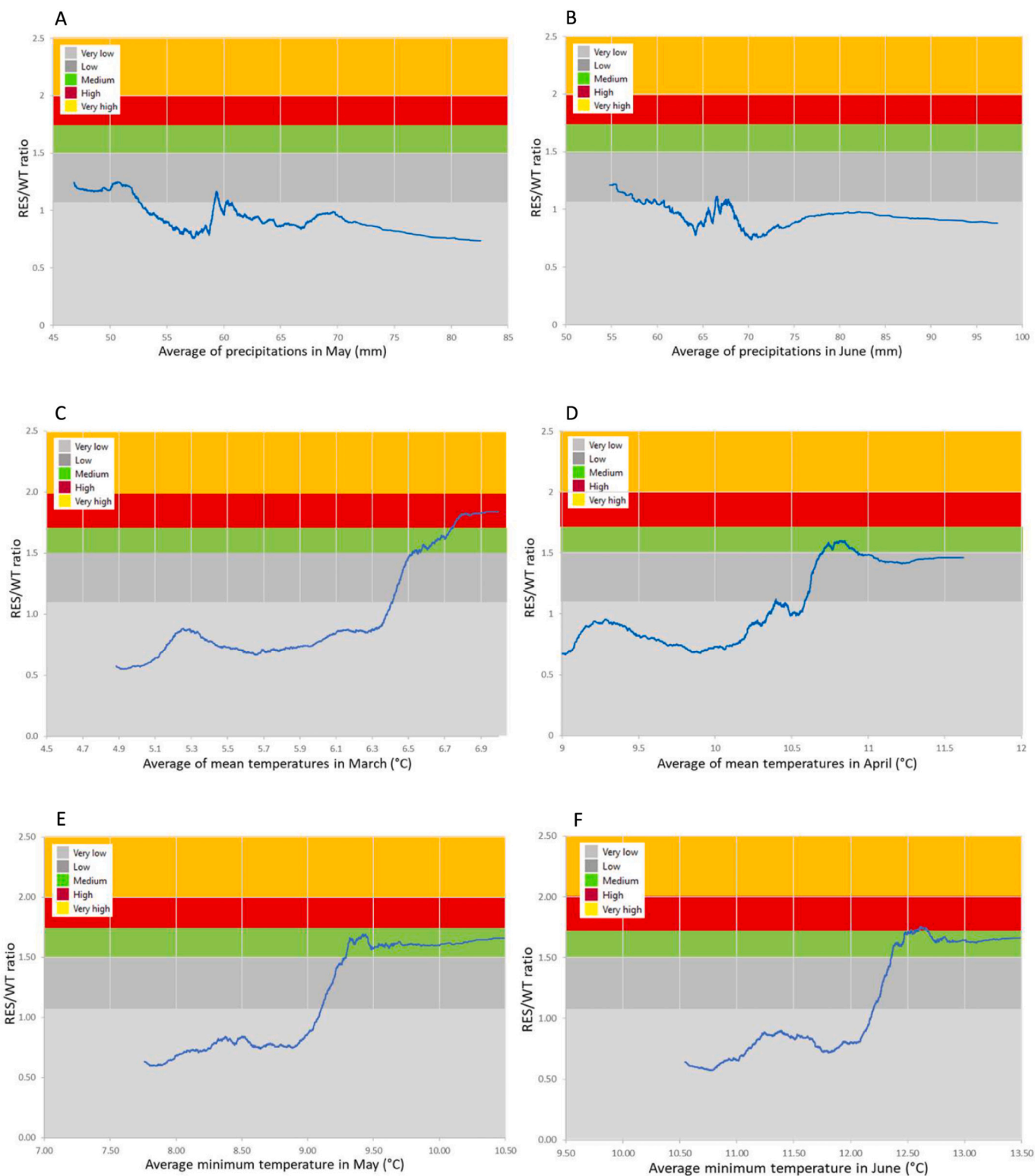


Fig. 6. Trend of the RES/WT ratio in relationship of A-B) precipitations in May and June, C–D) average temperatures in March and April, and E-F) minimum temperatures in May and June. Different colors are associated with the different risk classes.

these crops require minimal fungicide application. The relatively low concentration of azole fungicides in these soils may provide a more favorable environment for selection of azole resistant strains compared to soils with higher concentration. Furthermore, a recent study showed that some *A. fumigatus* azole resistant strains, compared to wild-type strains, presented a higher competitive fitness when exposed to azole-

free environments. These results suggested the existence of multiple genetic factors, other than *CYP51A* mutations, that are relevant for emergence and dispersion of mutants in the environment (Chen et al., 2024).

Legume plants are particularly resistant to pathogen attacks due to their ability to release of a variety of secondary metabolites, named

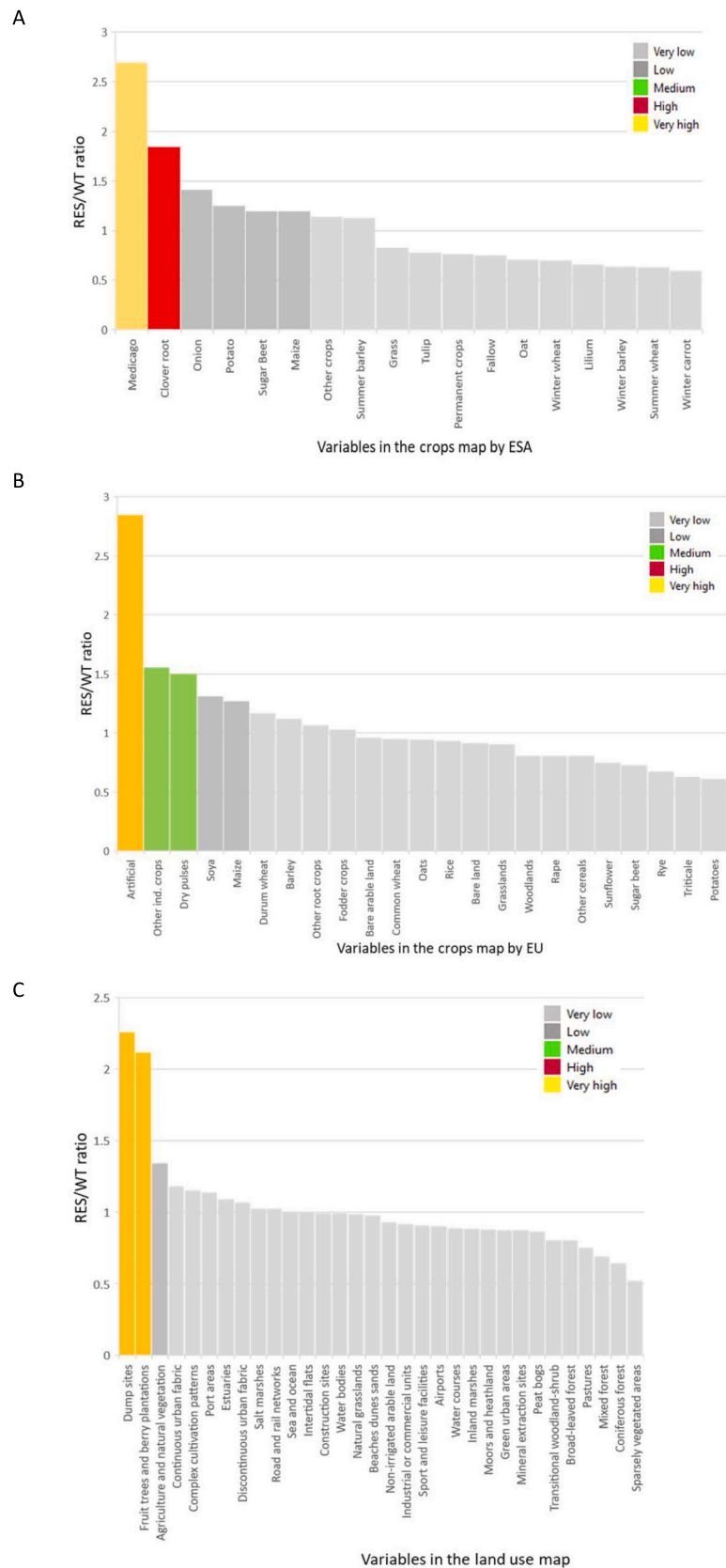
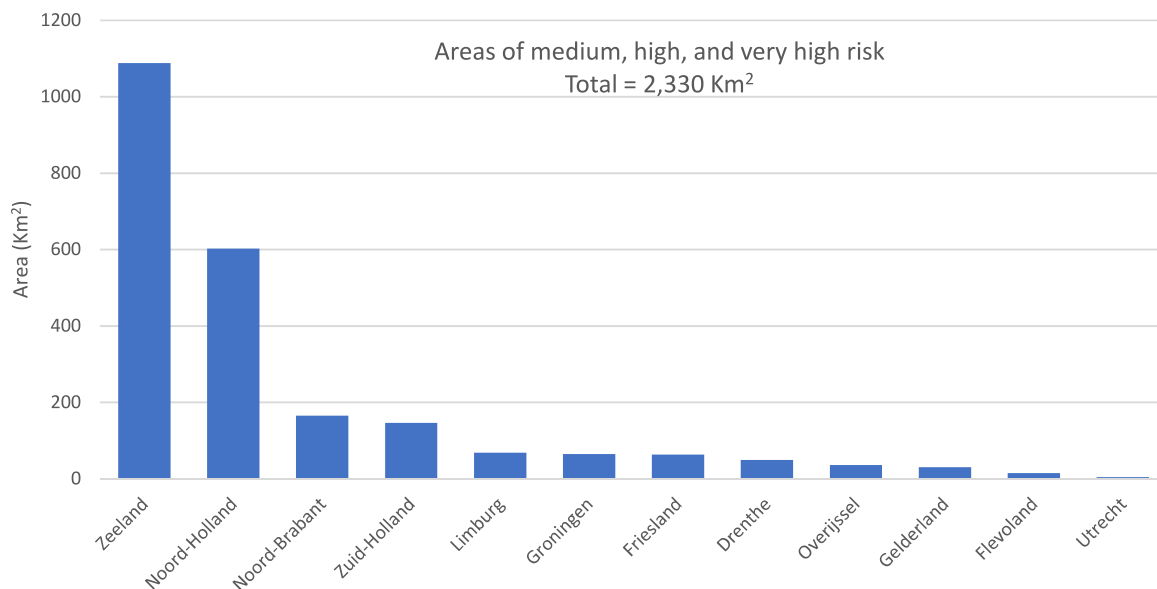


Fig. 7. Values of RES/WT for the categorical variables included in A) ESA crops map, B) EU crops map, and C) land use map. Different colors are associated with the different risk classes.

A



B

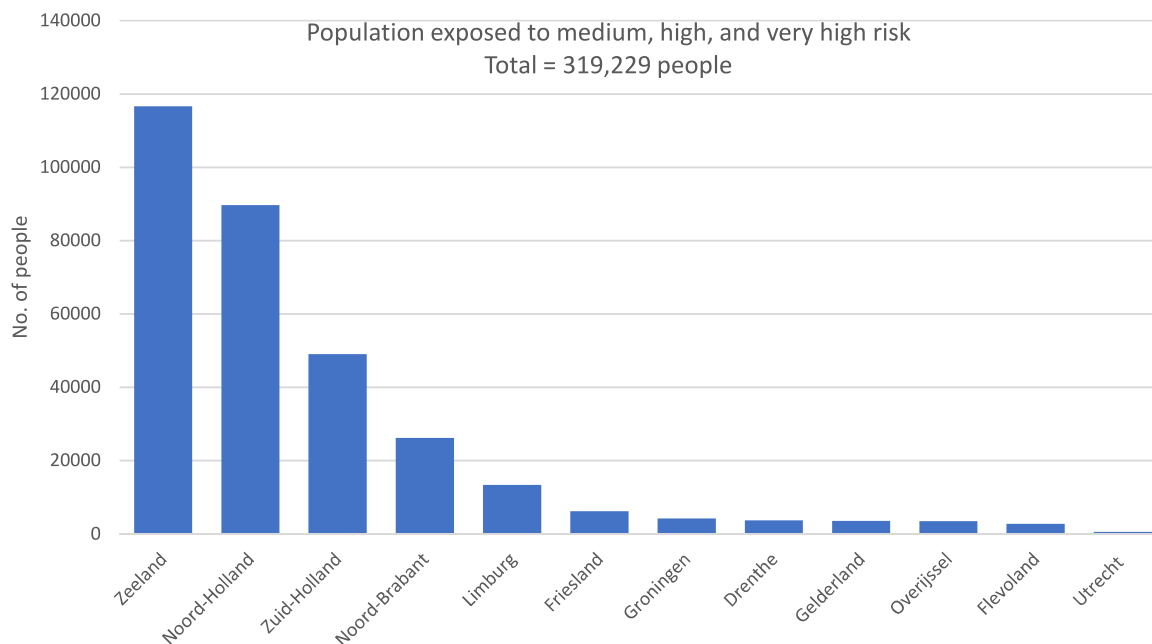


Fig. 8. A) Size of the Netherlands areas exposed to medium, high, and very high risk grouped by province. B) Number of people exposed to medium, high, and very high risk grouped by province.

phytoalexins, presenting anti-bacterial and anti-fungal properties (Liu et al., 2023). Resveratrol is an example of metabolite belonging to this category which was recently shown to be a powerful antifungal agent with synergic activity combined with azole drugs (Wang et al., 2021). The production of such metabolites by legumes could enhance the

selection of azole-resistant mutants in the soil, which might then advantage them over wild-types due to a better competitive fitness.

Our analysis was not able to find a direct correlation between the quantity of azole fungicides used in agriculture and the likelihood of observing aspergillosis cases due to resistant strains rather than wild-

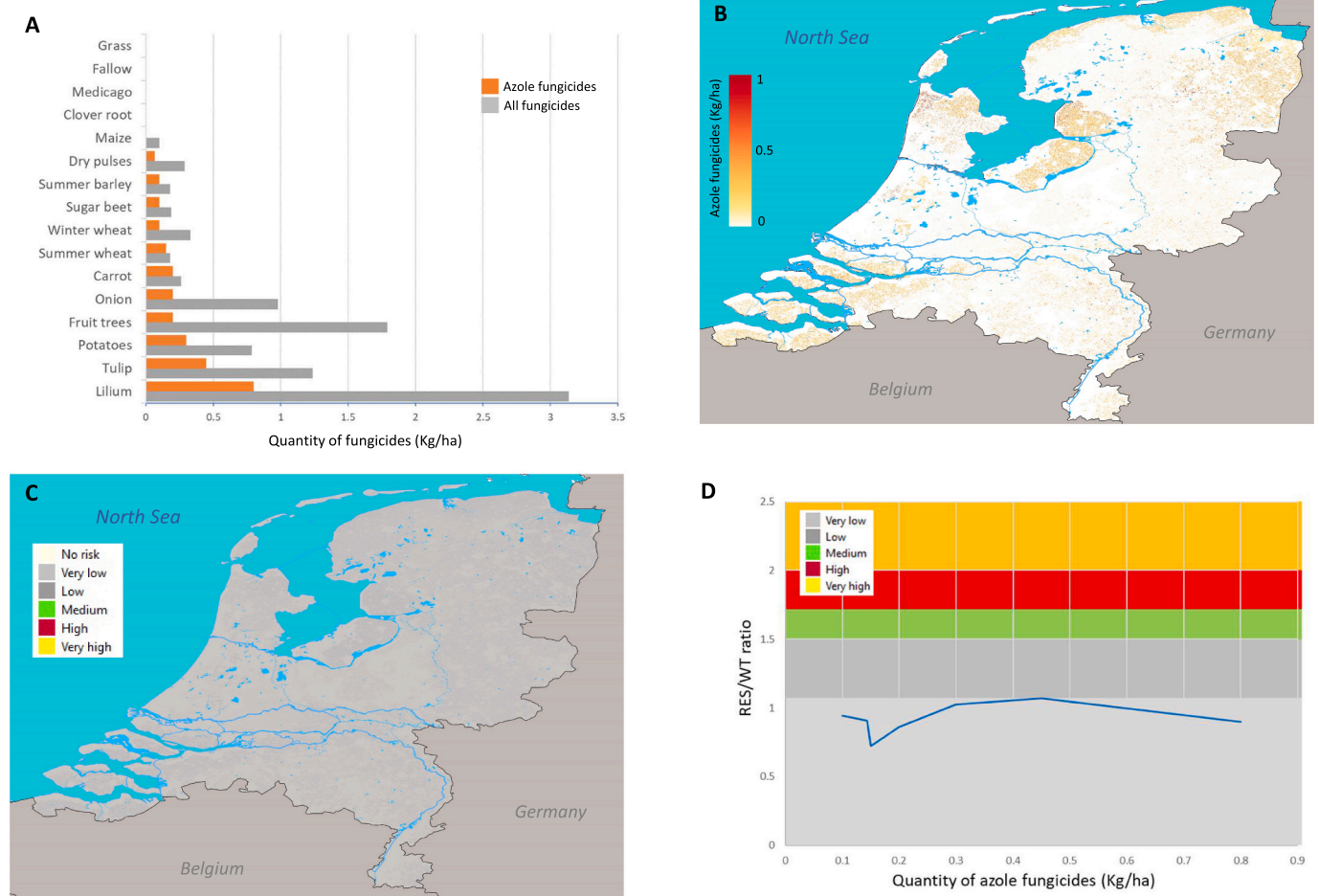


Fig. 9. A) Quantity of azole fungicides and total fungicides (kg/ha) used in the Netherlands to treat the different crops (data from Centraal Bureau voor de Statistiek). B) Inferred map showing the areas where azole fungicides are mostly employed. C) Distribution map inferred calculating the ratio between RES and WT distribution probabilities. D) Trend of the RES/WT ratio in relationship of azole quantity used to treat crops. Different colors are associated with the different risk classes.

type strains. These results could be attributed by the biases in the data recording, as mentioned in the previous section, or it may reflect a more complex picture where azole fungicides are not the sole environmental stress causing the emergence of resistant strains (Hollomon, 2017). The present study lends support to the latter hypothesis, as it identified a set of climatic and anthropogenic factors that were strongly correlated with high-risk areas. This is consistent with recent genomic-based studies that have drawn similar conclusions (Khateb et al., 2023; He et al., 2024; Chen et al., 2024).

The present study also explored the potential routes and directions of dispersion for the main *A. fumigatus* azole-resistant mutants in the Netherlands. The results revealed that the origin of these strains was most likely in the central area of the country corresponding to the area where the highest number of aspergillosis cases, both due to resistant or wild-type strains, were recorded. However, this area was classified by our prediction model as a very low risk area. A possible explanation for these results might be that the environmental factors in this area support the high proliferation of both wild-type and resistant strains, leading to a similar likelihood of infection by either type and thus resulting in a risk index (RES/WT ratio) of ≤ 1 . Conversely, areas such as Noord-Holland, Zeeland, Noord Brabant, and Limburg, which are farther from the source of dispersal, may have more favorable conditions for the competitive fitness of resistant strains compared to wild-type strains. In addition, despite resistant strains seems to expand also towards the north and the east of the country, it is likely that these areas are not suitable for high proliferation of resistant strains since the calculated risk index is low.

5. Conclusions

This study showed that climatic factors contributed more consistently than anthropogenic factors to the predictive distribution model suggesting that the actual global warming trend could have an impact on the emergence of antifungal resistance in future. Association of high-risk zones with agricultural practices such as orchards and greenhouses, seems to be in line with the hypothesis that the use of azole fungicides is responsible of the emergence of *A. fumigatus* azole resistance. However, the same association was also found with legume cultivations and dump sites where the use of fungicide is very limited. All together these results suggest that azole-resistance emergence is a complex phenomenon depending on a multitude of environmental variables that are not yet been fully explored.

Supplementary data to this article can be found online at <https://doi.org/10.1016/j.scitotenv.2024.177923>.

CRedit authorship contribution statement

Massimo Cogliati: Writing – review & editing, Writing – original draft, Supervision, Methodology, Formal analysis, Data curation, Conceptualization. **Jochem B. Buil:** Writing – review & editing, Data curation. **Maria Carmela Esposito:** Writing – review & editing. **Anna Prigitano:** Writing – review & editing. **Luisa Romanò:** Writing – review & editing. **Willem J.G. Melchers:** Writing – review & editing, Data curation.



Fig. 10. The Netherlands map showing the four predicted dispersion routes for TR34/L98H *Aspergillus fumigatus* resistant mutants. Different risk zones are identified with different colors. Province boundaries are also shown.

Declaration of competing interest

The authors declare that they have no known competing financial interests or personal relationships that could have appeared to influence the work reported in this paper.

Data availability

Data will be made available on request.

References

- Amona, F.M., Oladele, R.O., Resendiz-Sharp, A., Denning, D.W., Kosmidis, C., Lagrou, K., Zhong, H., Han, L., 2022. Triazole resistance in *Aspergillus fumigatus* isolates in Africa: a systematic review. *Med. Mycol.* 60, myac059.
- Arendrup, M.C., Hare, R.K., Jørgensen, K.M., Bollmann, U.E., Bech, T.B., Hansen, C.C., Heick, T.M., Jørgensen, L.N., 2024. Environmental hot spots and resistance-associated application practices for azole-resistant *Aspergillus fumigatus*, Denmark, 2020–2023. *Emerg. Infect. Dis.* 30, 1531–1541.
- Bongomin, F., Gago, S., Oladele, R.O., Denning, D.W., 2017. Global and multi-national prevalence of fungal diseases—estimate precision. *J. Fungi (Basel)* 3, 57.
- Bosetti, D., Neofytos, D., 2023. Invasive aspergillosis and the impact of azole-resistance. *Curr. Fungal Infect. Rep.* Mar 18, 1–10.
- Celia-Sanchez, B.N., Mangum, B., Gómez Londoño, L.F., Wang, C., Shuman, B., Brewer, M.T., Momany, M., 2024. Pan-azole- and multi-fungicide-resistant *Aspergillus fumigatus* is widespread in the United States. *Appl. Environ. Microbiol.* 90, e0178223.
- Chen, S., Zhu, G., Lin, H., Guo, J., Deng, S., Wu, W., Goldman, G.H., Lu, L., Zhang, Y., 2024. Variability in competitive fitness among environmental and clinical azole-resistant *Aspergillus fumigatus* isolates. *mBio* 15, e0026324.
- Chowdhary, A., Sharma, C., Kathuria, S., Hagen, F., Meis, J.F., 2013. Emergence of multi triazole-resistant *Aspergillus fumigatus* carrying the TR46/Y121F/T289A mutations in cyp51A gene from Indian environment. *Mycoses* 56, 69.
- De Francesco, M.A., 2023. Drug-resistant *Aspergillus* spp.: a literature review of its resistance mechanisms and its prevalence in Europe. *Pathogens* 12, 1305.
- Fisher, M.C., Hawkins, N.J., Sanglard, D., Gurr, S.J., 2018. Worldwide emergence of resistance to antifungal drugs challenges human health and food security. *Science* 360, 739–742.
- Godeau, C., Morin-Crini, N., Crini, G., Guillemin, J.P., Voisin, A.S., Dousset, S., Rocchi, S., 2023. Field-crop soils in eastern France: coldspots of azole-resistant *Aspergillus fumigatus*. *J. Fungi (Basel)* 9, 618.
- Gómez Londoño, L.F., Brewer, M.T., 2023. Detection of azole-resistant *Aspergillus fumigatus* in the environment from air, plant debris, compost, and soil. *PLoS One* 18, e0282499.
- Hanne D, Philippe C, Karine G, Paulien L, Jessie C, De Elien V, Marc V, Liesbet B, Charlotte B, Claude S, Ann P. Detection of pan-azole resistant *Aspergillus fumigatus* in horticulture and a composting facility in Belgium. *Med Mycol* 2024;May 20: myae055.
- He, X., Kusuya, Y., Hagiwara, D., Toyotome, T., Arai, T., Bian, C., Nagayama, M., Shibata, S., Watanabe, A., Takahashi, H., 2024. Genomic diversity of the pathogenic fungus *Aspergillus fumigatus* in Japan reveals the complex genomic basis of azole resistance. *Commun. Biol.* 7, 274.
- Heylen, J., Vanbiervliet, Y., Maertens, J., Rijnders, B., Wauters, J., 2024. Acute invasive pulmonary aspergillosis: clinical presentation and treatment. *Semin. Respir. Crit. Care Med.* 45, 69–87.
- Hollomon, D., 2017. Does agricultural use of azole fungicides contribute to resistance in the human pathogen *Aspergillus fumigatus*? *Pest Manag. Sci.* 73, 1987–1993.
- Kang SE, Sumabat LG, Melie T, Mangum B, Momany M, Brewer MT. Evidence for the agricultural origin of resistance to multiple antimicrobials in *Aspergillus fumigatus*, a fungal pathogen of humans. *G3 (Bethesda)* 2022;12:jkab427.
- Kemoi, E.K., Nyerere, A., Gross, U., Bader, O., Gono, T., Bii, C., 2017. Diversity of azoles resistant *Aspergillus* species isolated from experience and naïve soils in Nairobi county and Naivasha sub-county Kenya. *Eur. Sci. J.* 13, 301.
- Khateb, A., Gago, S., Bromley, M., Richardson, M., Bowyer, P., 2023. Aneuploidy is associated with azole resistance in *Aspergillus fumigatus*. *Antimicrob. Agents Chemother.* 67, e0125322.
- Kontro, M.H., Kirsi, M., Laitinen, S.K., 2022. Exposure to bacterial and fungal bioaerosols in facilities processing biodegradable waste. *Front. Public Health* 10, 789861.

- Korfanty, G.A., Dixon, M., Jia, H., Yoell, H., Xu, J., 2021. Genetic diversity and dispersal of *Aspergillus fumigatus* in arctic soils. *Genes* (Basel) 13, 19.
- Kwon-Chung, K.J., Sugui, J.A., 2013. *Aspergillus fumigatus* - what makes the species a ubiquitous human fungal pathogen? *PLoS Pathog.* 9, e1003743.
- Lin H, Guo J, Li Y, Xiao C, Hu L, Chen H, Lu X, Wu W. In vitro antifungal susceptibility profile and genotypic characterization of clinical *Aspergillus* isolates in Eastern China on behalf of Eastern China Invasive Fungi Infection Group. *Med Mycol* 2023;61: myad082.
- van der Linden, J.W., Snelders, E., Kampinga, G.A., Rijnders, B.J., Mattsson, E., Debets-Ossenkopp, Y.J., Kuijper, E.J., Van Tiel, F.H., Melchers, W.J., Verweij, P.E., 2011. Clinical implications of azole resistance in *Aspergillus fumigatus*, the Netherlands, 2007-2009. *Emerg. Infect. Dis.* 17, 1846-1854.
- Liu, J.C., Yang, J., Lei, S.X., Wang, M.F., Ma, Y.N., Yang, R., 2023. Natural phytoalexins inspired the discovery of new biphenyls as potent antifungal agents for treatment of invasive fungal infections. *Eur. J. Med. Chem.* 261, 115842.
- Lockhart, S.R., Chowdhary, A., Gold, J.A.W., 2023. The rapid emergence of antifungal-resistant human-pathogenic fungi. *Nat. Rev. Microbiol.* 21, 818-832.
- Phillips, S.J., Anderson, R.P., Schapire, R.E., 2006. Maximum entropy modeling of species geographic distributions. *Ecol. Model.* 190, 231-259.
- Prigitano, A., Venier, V., Cogliati, M., De Lorenzis, G., Esposto, M.C., Tortorano, A.M., 2014. Azole-resistant *Aspergillus fumigatus* in the environment of northern Italy, may 2011 to June 2012. *Euro Surveill.* 19, 20747.
- Pugliese, M., Matic, S., Prethi, S., Gisi, U., Gullino, M.L., 2018. Molecular characterization and sensitivity to demethylation inhibitor fungicides of *Aspergillus fumigatus* from orange-based compost. *PLoS One* 13, e0200569.
- Schoustra, S.E., Debets, A.J.M., Rijs, A.J.M.M., Zhang, J., Snelders, E., Leendertse, P.C., Melchers, W.J.G., Rietveld, A.G., Zwaan, B.J., Verweij, P.E., 2019. Environmental hotspots for azole resistance selection of *Aspergillus fumigatus*, the Netherlands. *Emerg. Infect. Dis.* 25, 1347-1353.
- Shelton, J.M.G., Collins, R., Uzzell, C.B., Alghamdi, A., Dyer, P.S., Singer, A.C., Fisher, M. C., 2022. Citizen science surveillance of triazole-resistant *Aspergillus fumigatus* in United Kingdom residential garden soils. *Appl. Environ. Microbiol.* 88, e0206121.
- Shelton, J.M.G., Rhodes, J., Uzzell, C.B., Hemmings, S., Brackin, A.P., Sewell, T.R., Alghamdi, A., Dyer, P.S., Fraser, M., Borman, A.M., Johnson, E.M., Piel, F.B., Singer, A.C., Fisher, M.C., 2023. Citizen science reveals landscape-scale exposures to multiazole-resistant *Aspergillus fumigatus* bioaerosols. *Sci. Adv.* 9, eadh8839.
- Snelders, E., van der Lee, H.A., Kuijpers, J., Rijs, A.J., Varga, J., Samson, R.A., Mellado, E., Donders, A.R., Melchers, W.J., Verweij, P.E., 2008. Emergence of azole resistance in *Aspergillus fumigatus* and spread of a single resistance mechanism. *PLoS Med.* 5, e219.
- Toda, M., Beer, K.D., Kuivila, K.M., Chiller, T.M., Jackson, B.R., 2021. Trends in agricultural triazole fungicide use in the United States, 1992-2016 and possible implications for antifungal-resistant fungi in human disease. *Environ. Health Perspect.* 129, 55001.
- Verweij, P.E., Snelders, E., Kema, G.H., Mellado, E., Melchers, W.J., 2009. Azole resistance in *Aspergillus fumigatus*: a side-effect of environmental fungicide use? *Lancet Infect. Dis.* 9, 789-795.
- Wang, C., Miller, N., Vines, D., Severns, P.M., Momany, M., Brewer, M.T., 2024. Azole resistance mechanisms and population structure of the human pathogen *Aspergillus fumigatus* on retail plant products. *Appl. Environ. Microbiol.* 90, e0205623.
- Wang, J., Zhang, X., Gao, L., Wang, L., Song, F., Zhang, L., Wan, Y., 2021. The synergistic antifungal activity of resveratrol with azoles against *Candida albicans*. *Lett. Appl. Microbiol.* 72, 688-697.
- WHO. WHO Fungal Priority Pathogens List to Guide Research, Development, and Public Health Action. 2022. <https://www.who.int/publications/i/item/9789240060241>.
- Zhang, J., Lopez Jimenez, L., Snelders, E., Debets, A.J.M., Rietveld, A.G., Zwaan, B.J., Verweij, P.E., Schoustra, S.E., 2021. Dynamics of *Aspergillus fumigatus* in azole fungicide-containing plant waste in the Netherlands (2016-2017). *Appl. Environ. Microbiol.* 87, e02295-20.
- Zhou, D., Korfanty, G.A., Mo, M., Wang, R., Li, X., Li, H., Li, S., Wu, J.Y., Zhang, K.Q., Zhang, Y., Xu, J., 2021. Extensive genetic diversity and widespread azole resistance in greenhouse populations of *Aspergillus fumigatus* in Yunnan, China. *mSphere* 6, e00066-21.
- Zhou, D., Wang, R., Li, X., Peng, B., Yang, G., Zhang, K.Q., Zhang, Y., Xu, J., 2022. Genetic diversity and azole resistance among natural *Aspergillus fumigatus* populations in Yunnan, China. *Microb. Ecol.* 83, 869-885.
- Zhou D, Gong J, Duan C, He J, Zhang Y, Xu J. Genetic structure and triazole resistance among *Aspergillus fumigatus* populations from remote and undeveloped regions in Eastern Himalaya. *mSphere* 2023;8:e0007123.